Comparative study of the vanadium species in VAPO-5 and VAPSO-5 molecular sieves

ARTICLE *in* THE JOURNAL OF PHYSICAL CHEMISTRY B · AUGUST 2002

Impact Factor: 3.3 · DOI: 10.1021/jp013285q

Comparative Study of the Vanadium Species in VAPO-5 and VAPSO-5 Molecular Sieves

Jianqiang Yu, Meijun Li, Zhongmin Liu, Zhaochi Feng, Qin Xin, and Can Li*

State Key Laboratory of Catalysis, Dalian Institute of Chemical Physics, Chinese Academy of Sciences, P.O. Box 110, Dalian 116023, China

Received: August 24, 2001; In Final Form: January 29, 2002

By using XRD, TG-DTA, NMR, and UV resonance Raman spectroscopy, the nature and location of vanadium species between VAPO-5 and VAPSO-5 molecular sieves were comparatively studied. It was found that different vanadium species exist in VAPO-5 and VAPSO-5 molecular sieves. Polymerized vanadium oxides and bulk V_2O_5 crystallites are the main vanadium species in VAPO-5 molecular sieves. However, in VAPSO-5 molecular sieves, tetrahedrally coordinated vanadium species are dominant. Namely, most of the vanadium species in VAPO-5 exist outside the framework, whereas most of the vanadium species in VAPSO-5 are incorporated into the framework. The formation of framework vanadium in VAPSO-5 molecular sieves is found to be associated essentially with the presence of framework silicon atoms.

Introduction

The study of crystalline aluminophosphates ($AlPO_4$-n) is an interesting topic because of the potential use of these materials as adsorbents and heterogeneous catalysts both in industry and in foundational research.[1] An attractive property of these materials is that their Al or P atoms can be substituted by silicon atoms to form SAPO-n (where n denotes a particular structure type) and also by other metals to form MeAPO/MeAPSO materials.[2−4] MeAPO and MeAPSO molecular sieves constitute a new class of catalysts having both acid sites and metal redox properties in microporous environments. The incorporated metal ions often show special catalytic activities that are different from those observed for metal ions residing in ion-exchanged sites inside the channels or cages of a molecular sieve or for a simple physical mixture of a metal oxide and a molecular sieve. Synthesis of metal-incorporated aluminophosphate and silicoaluminophosphate molecular sieves (MeAPO/MeAPSO) was first reported in 1986.[5,6] The metal ion, Me, can be the ion of either a transition metal such as Ti, V, Cr, Mn, Co, or Ni or a nontransition metal such as Mg. The unique catalytic properties of these materials have been demonstrated for several reactions.[7−10]

Metal-containing aluminophosphate has been studied by various physicochemical methods including IR, UV−vis, electron spin resonance (ESR), electron spin−echo modulation (ESEM), Mössbauer, X-ray photoelectron, X-ray absorption (EXAFS and XANES) spectroscopies, ^{27}Al, ^{29}Si, and ^{31}P MAS NMR, scanning electron microscopy, energy dispersive analysis of X-rays (EDAX), chemical analysis, measurement of acidity by temperature-programmed ammonia desorption, test of sorption and ion-exchange capacity, catalytic test reactions, and powder and single-crystal diffraction methods.[11,12] Although these methods do not directly probe the local environment of the metal ion, the results support the idea that highly isolated or dispersed metal ions can be incorporated into molecular sieves under controlled synthesis procedures.

The introduction of two kinds of ions such as Mg and V, Si and V, or Ti and V into the $AlPO_4$-5-type structure to give VMgAPO-5, VAPSO-5, or VTAPO-5 has also been reported. Among them, the introduction of V into $AlPO_4$-n molecular sieves to form VAPO-n and the introduction of V and Si into $AlPO_4$-n molecular sieves to form VAPSO-n have received much more attention because these VAPO and VAPSO molecular sieves show special catalytic properties in the selective oxidation of hydrocarbons.[13−19] VAPO and VAPSO molecular sieves have different acidic properties, which can influence the catalytic performance. However, the different catalytic behaviors of VAPO and VAPSO are also mainly related to the different vanadium species inside the channel or in the framework. The catalytic properties of transition metal ions incorporated into molecular sieves are strongly dependent on the nature and location of the metal ions and on their accessibility to and coordination with adsorbate molecules. Thus, the identification of the location and coordination of the vanadium atoms in the molecular sieves is important in understanding the chemistry of VAPO and VAPSO catalysts. Although many modern physicochemical method studies have been used to investigate the vanadium species existing in VAPO-5 and VAPSO-5 catalysts, many uncertainties concerning the location and coordination of the vanadium species in the zeolites remain.

In this work, we have used XRD, TG-DTA, NMR, and UV resonance Raman spectroscopy to compare the differences in the nature, coordination state, and location of vanadium species between VAPO-5 and VAPSO-5 molecular sieves. We found that the framework vanadium ions are formed in VAPSO-5 but are difficult to form in VAPO-5 and that the silicon ions in VAPO-5 play an important role in the formation of framework vanadium species.

Experimental Section

Synthesis. VAPO-5 and VAPSO-5 molecular sieves were synthesized hydrothermally. Phosphoric acid (85%), pseudoboehmite (78.18% Al_2O_3), colloidal silica (25.5 wt %), and $VOSO_4 \cdot 3H_2O$ were used as the sources for phosphorus, aluminum, silicon, and vanadium, respectively. The composi-

* To whom correspondence should be addressed. E-mail: canli@dicp.ac.cn. Tel: 86-411-4671991 ext. 728, 726. Fax +86-411-4694447. Homepage: http://www.canli.dicp.ac.cn.

10.1021/jp013285q CCC: $22.00
Published on Web 08/10/2002

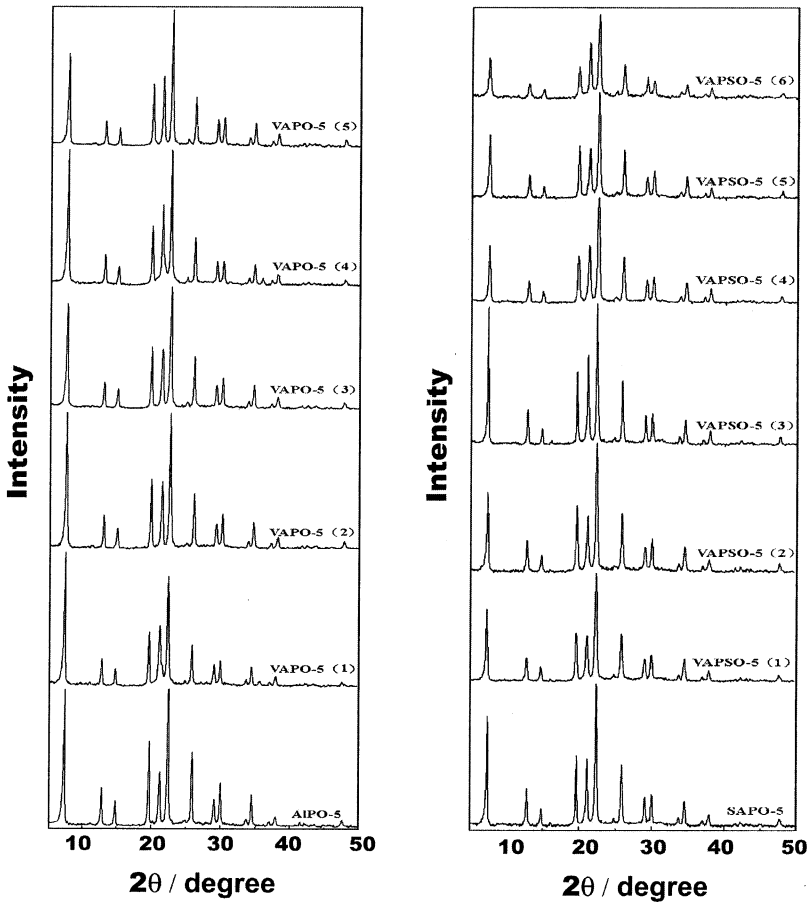

Figure 1. XRD patterns of VAPO-5 and VAPSO-5 with increasing vanadium content.

tions of the synthesis gels are $Al_2O_3/P_2O_5/xV_2O_5/1.35Et_3N/40H_2O$ ($x = 0-0.1$) for VAPO-5 and $Al_2O_3/P_2O_5/0.6SiO_2/xV_2O_5/1.35Et_3N/40H_2O$ ($x = 0-0.1$) for VAPSO-5. The synthesis procedures are as follows: A solution of phosphoric acid and water in a 3:5 weight ratio was added to an aqueous suspension of pseudoboehmite powder (72.18 wt % Al_2O_3), followed by violent stirring for 2 h. Then a mixture of colloidal silica and aqueous $VOSO_4$ was added dropwise for the synthesis of VAPSO-5 whereas only aqueous $VOSO_4$ was added for the synthesis of VAPO-5. After stirring for another 2 h, the organic template triethylamine was added, and the mixture was stirred until a homogeneous gel was formed. The resultant mixture was transferred to an autoclave and crystallized at 180 °C for 24 h. The products were washed with deionized water, filtered, and dried at 100 °C and were then calcined at 550 °C for 5 h.

Characterization. X-ray power diffraction was measured on a Rigaku D/MAX-rb diffractometer employing Ni-filtered Cu Kα radiation ($\lambda = 1.5404$ Å). Thermogravimetric (TG) analysis and differential thermal analysis (DTA) were performed on a TGS-2 and a DTA-1700 in the temperature range of 30−800 °C with a 0.02 g sample. NMR spectra were recorded at ambient temperature on a Bruker DRX-400 spectrometer. The spinning speeds were 4, 8, and 4.3 KHz. UV−Raman spectra were recorded on a homemade UV−Raman spectrometer.[20−22] A 244-nm line from an Innova 300 FRED (Coherent) laser was used as the excitation source.

Results

Synthesis. XRD powder patterns of VAPO-5 and VAPSO-5 with different vanadium contents are shown in Figure 1. The patterns are typical features for the $AlPO_4$-5 structure,[23] but the relative intensity of the peaks depends on the vanadium content. No bulk vanadium pentoxide phase is present because the characteristic peaks of vanadium pentoxide at $2\theta = 15.5$, 20.3, 21.9, and 31.0°, which are clearly distinguished from the peaks of $AlPO_4$-5, are not observed in the XRD patterns of VAPO-5 and VAPSO-5. Table 1 and Table 2 give the gel composition in the synthesis of VAPO-5 and VAPSO-5 and the relative crystallinity of the as-synthesized and calcined VAPO-5 and VAPSO-5 samples. It can be seen from the Tables that the calcination of VAPO-5 and VAPSO-5 leads to a decrease in their relative crystallinity. By comparing the crystallinity of VAPO-5 with that of $AlPO_4$-5 and of VAPSO-5 with that of SAPO-5, it can be seen that the introduction of vanadium decreases the degree of crystallinity, whereas the crystallinity of VAPSO-5 first increases to a maximum and then decreases with increasing vanadium content. The different trend in the relative crystallinity reflects the fact that the relative crystallinity of VAPO-5 and VAPSO-5 depends on the composition of the samples. Furthermore, Tables 1 and 2 also show that pure phases of VAPO-5 and VAPSO-5 can be synthesized with a relatively high content of vanadium in the synthesis gel. However, the stability of the crystals after the calcination depends on the vanadium content. The structure of VAPO-5 is stable only when the V/P atomic ratio is below 0.05, whereas the structure of VAPSO-5 can be stable for V/P atomic ratios up to 0.1. It is obvious that the addition of Si in the synthesis gel may increase the stability of the framework of the calcined sample. When the vanadium content increases to a value that is higher than these limits, the structures of VAPO-5 and VAPSO-5 are not stable, the AFI phase collapses, and tridimite-type and V_2O_5 crystallites are formed upon calcination at high temperatures.

TABLE 1: Gel Compositions, Crystallization, and Crystallinity of VAPO-5

	gel composition: $xV_2O_5/(1-x)Al_2O_3/P_2O_5/yNEt_3/40H_2O$			relative crystallization (%)	
samples	x	y	crystallization temperature (°C)	as-synthesized	calcined
$AlPO_4$-5	0	1.35	180	100	73
VAPO-5 (1)	0.0025	1.35	180	92	57
VAPO-5 (2)	0.005	1.35	180	67	69
VAPO-5 (3)	0.01	1.35	180	94	62
VAPO-5 (4)	0.03	1.35	180	84	69
VAPO-5 (5)	0.05	1.35	180	90	68
VAPO-5 (6)	0.075	1.35	180	77	tridymite + V_2O_5
VAPO-5 (7)	0.1	1.35	180	74	tridymite + V_2O_5
VAPO-5 (8)	0.2	1.35	180	61	tridymite + V_2O_5
VAPO-5 (9)	0.3	1.35	180		tridymite + V_2O_5

TABLE 2: Gel Compositions, Crystallization Temperature, and Crystallinity of VAPSO-5

	gel composition: $xV_2O_5/zSiO_2/(1-x)Al_2O_3/P_2O_5/yNEt_3/4H_2O$				relative crystallization (%)	
samples	x	y	z	crystallization temperature (°C)	as-synthesized	calcined
SAPO-5	0	1.35	0.6	180	85	70
VAPSO-5 (1)	0.05	1.35	0.6	180	86	50
VAPSO-5 (2)	0.01	1.35	0.6	180	85	61
VAPSO-5 (3)	0.02	1.35	0.6	180	90	78
VAPSO-5 (4)	0.03	1.35	0.6	180	100	52
VAPSO-5 (5)	0.05	1.35	0.6	180	84	51
VAPSO-5 (6)	0.1	1.35	0.6	180	79	44
VAPSO-5 (7)	0.2	1.35	0.6	180	64	tridymite + V_2O_5

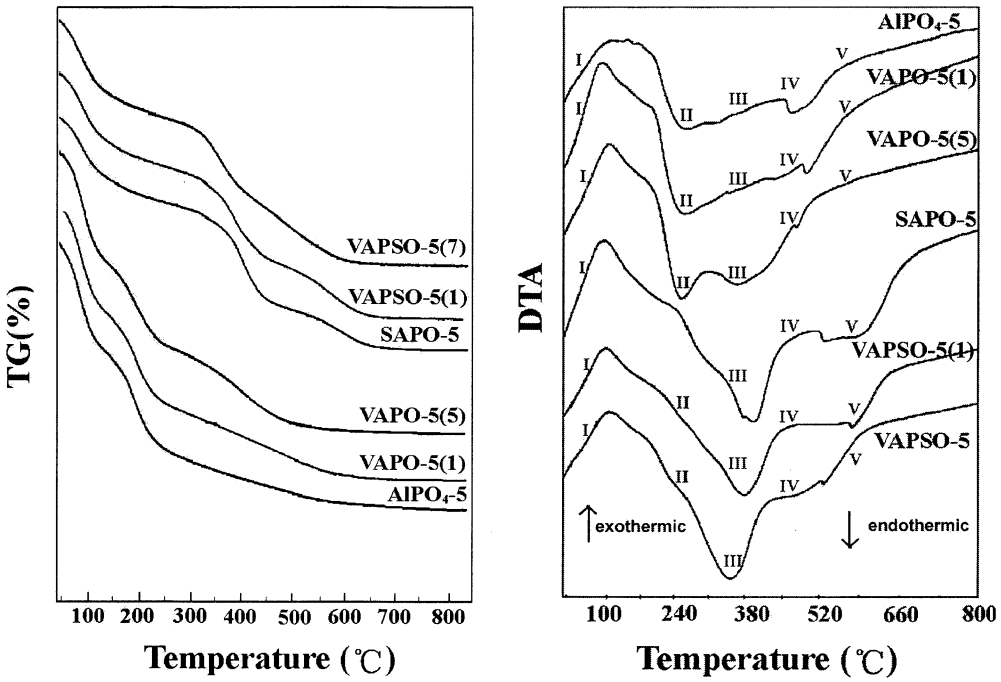

Figure 2. TG and DTA profile of VAPO-5 and VAPSO-5.

The VAPO-5 and VAPSO-5 samples are greenish white before the calcination treatment. Upon calcination, the color of the VAPO-5 samples turns to yellow, whereas the color of the VAPSO-5 samples turns to white. We know that different valences and coordinations of vanadium ions exhibit different colors. Thus, although this is only an original vision phenomenon, it also indicates that the coordination states of the vanadium species in VAPO-5 and VAPSO-5 are different from each other.

Thermal Analysis. The thermal properties of as-synthesized $AlPO_4$-5, SAPO-5, VAPO-5, and VAPSO-5 were investigated by thermal analysis in flowing O_2. The TG and DTA profiles are shown in Figure 2. In the TG profiles, three different weight losses were detected in the three temperature ranges: 30−80, 80−240, and 240−630 °C. The first two steps correspond to endothermic processes in which the low-temperature step is due to water desorption and the second step is due to desorption of triethylamine occluded inside the channels. The third-step weight loss from 240−630 °C is assigned to the desorption and decomposition of protonated amines. When comparing the TG profiles of VAPO-5 to that of $AlPO_4$-5, it can be seen that the curves are almost the same. Similarly, large differences were not found between the TG profiles of VAPSO-5 and SAPO-5. However, it is interesting that large differences between the TG profile of VAPSO-5 and VAPO-5 are observed, which suggests that the introduction the vanadium ions into $AlPO_4$-5 and

TABLE 3: TG/DTA Results of VAPO-5 and VAPSO-5

	organic weight loss (wt %)		
sample	endothermic	exothermic	total weight loss
AlPO-5	12.2	2.6	14.8
VAPO(1)	11.3	3.0	14.3
VAPO(5)	10.0	4.4	14.4
SAPO-5	4.7	7.5	12.2
VAPSO(1)	5.2	7.6	12.8
VAPSO(4)	5.6	7.2	12.8
VAPSO(7)	6.7	6.8	13.5

SAPO-5 exerts little influence on the desorption and decomposition of protonated amines, whereas the introduction of silicon atoms has a great influence. The fact that the desorption and decomposition of protonated amines is related to the framework charge explains why the amount of framework charge in the VAPO-5 and VAPSO-5 does not increase greatly with the addition of vanadium atoms but increases significantly with the addition of silicon.

The DTA curves reveal that the calcination process in air proceeds in five stages. Stage I shows the endothermic desorption of water. Stages II−IV, which are exothermic, reveal the oxidative decomposition of the template molecules. The diffusibility of the template during the calcination of the sample depends on the state of the template anchored inside the pore of the molecular sieves. If the template is in occluded form in the pores of $AlPO_4$-5, it is removed easily in stage II during the calcination. However, some template molecules interact strongly with the stronger acid sites of the sample and are not able to diffuse freely. These template molecules are removed at relatively higher temperatures. Stage V shows the combustion of coke. Certain amounts of the template are converted into coke during the calcination and can be burnt out in air during stage V at higher temperatures.

VAPO-5 shows a similar thermo-analytical curve to that of $AlPO_4$-5. Two main processes of the removal of the template are observed, which is in agreement with the result reported in the literature.[24,25] Stage III, which is associated with the strong Lewis acid sites induced by lattice defects, shows quite a difference. The sample with low vanadium content shows a similar peak to that of $AlPO_4$-5, whereas the sample shows more thermal exhaustion. This result suggests that two different types of the anchored mode for the template are present in VAPO-5 and that one may interact with the vanadium species.

For SAPO-5 and VAPSO-5, a more pronounced peak is observed in stage III, and only a weak shoulder peak appears in stage II, which illustrates that the amounts of pronated triethylamine in SAPO-5 and in VAPSO-5 molecular sieves are high and that the template is removed by combustion at high temperatures. Moreover, it is interesting that the exothermic peak of VAPSO-5 shifts to lower temperatures compared to that of SAPO-5; the more evident shift is observed for the sample with the higher content of vanadium. This result suggests that the charge in the framework has been changed with different vanadium content, which most probably is caused by isomorphous substitution.

The weight losses associated with template degradation in the different temperature ranges are listed in Table 3. It can be seen that the weight losses of VAPO-5 in the endothermic process are much more than those in the exothermic process, whereas the weight losses of VAPSO-5 in the two procedures are similar. However, the total organic content is approximately constant and is equal to ~14 wt % for the VAPO-5 sample and ~13.3 wt % for the VAPSO-5 samples. These values correspon

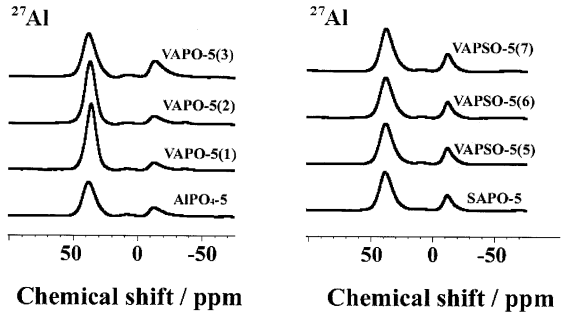

Figure 3. ^{27}Al MAS NMR spectra of VAPO-5 and VAPSO-5.

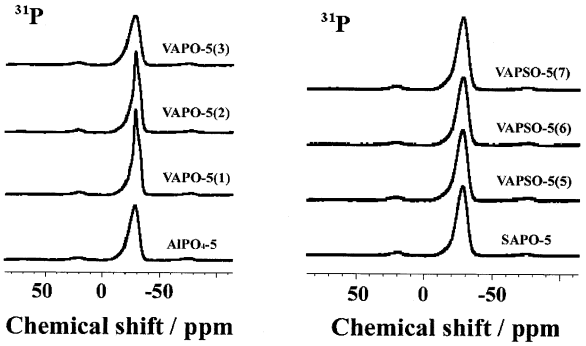

Figure 4. ^{31}P MAS NMR spectra of VAPO-5 and VAPSO-5.

to about 2.5 molecules of TEA per unit cell in VAPO-5 and 2.0 molecules of TEA per unit cell in VAPSO-5.

Solid-State NMR Spectra. Figures 3 and 4 present the ^{27}Al and ^{31}P MAS NMR spectra of calcined VAPO-5 and VAPSO-5 with varying amounts of vanadium. The ^{27}Al NMR spectra of VAPO-5 and VAPSO-5 are composed of three peaks at 36, 10 and −12 ppm. The main line at 36 ppm is ascribed to the tetrahedral aluminum in the aluminophosphate framework.[26,27] The peak at 10 ppm is assigned to the remaining pseudobohemite.[28] The resonance peak at −12 ppm is attributed to hexacoordinated Al. This kind of hexacoordinated aluminum is possibly formed upon water adsorption or possibly coordinated with vanadium species. It was often reported in the literature that in aluminophosphate molecular sieves the adsorption of water caused the appearance of resonance peaks in the pentacoordinated and octahedral regions of the ^{27}Al MAS NMR spectra.[29−32]

^{31}P NMR spectra of VAPO-5 and VAPSO-5 show a central band at around −29 ppm, with some asymmetry at low field. The broad resonance at ca. −29 ppm can be readily attributed to the tetrahedral phosphorus in a $P(O-Al)_4$ environment.[27,33−35] It is known that the ^{31}P resonance is considerably shifted because of the contact interaction of paramagnetic species. As an example, it has been reported that the signal of P(3Al, Mg) in the VMgAPO-5 sample is at −24 ppm, which illustrates that the differently coordinated environment of P atoms corresponds to a different resonance peak in the NMR spectra. However, the spectra of VAPO-5 and VAPSO-5 are much more similar to those of $AlPO_4$-5 and SAPO-5, respectively. Neither the shifts of the central peaks nor new resonance peaks are observed with the introduction of vanadium atoms, which suggests that only one kind of coordination mode of phosphorus exists in the framework of VAPO-5 and VAPSO-5. It also means that the coordination environment of P atoms may not be influenced by the addition of vanadium—that is to say that vanadium is not coordinated with P atoms in the framework.

^{28}Si MAS NMR spectra of SAPO-5 and VAPSO-5 with different contents of vanadium are shown in Figure 5. The

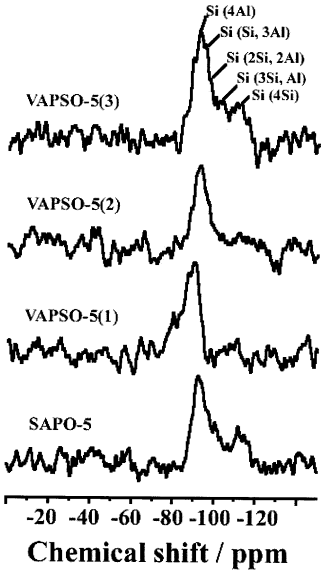

Figure 5. ^{28}Si MAS NMR spectra of SAPO-5 and VAPSO-5.

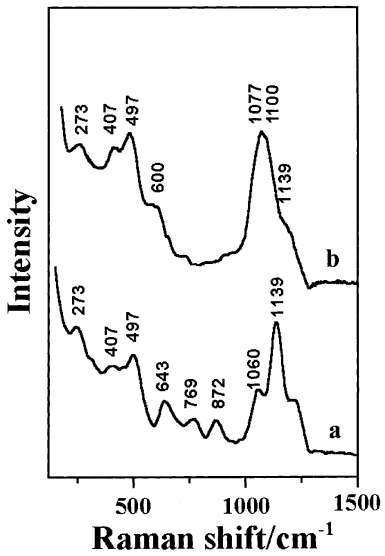

Figure 6. UV−Raman spectra of (a) $AlPO_4$-5 and (b) SAPO-5.

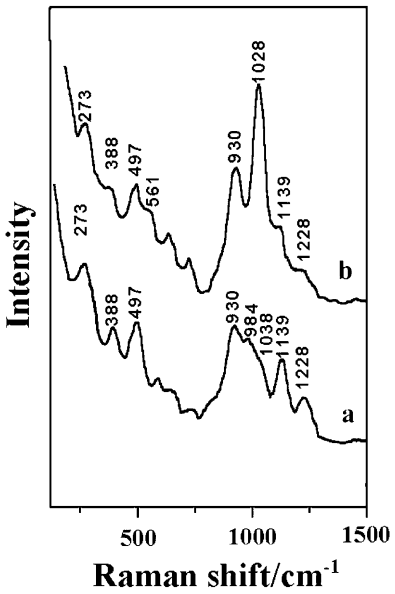

Figure 7. UV−Raman spectra of (a) VAPO-5 and (b) VAPSO-5.

spectrum of SAPO-5 consists of an intense peak at −91.6 ppm and three weak peaks at −96, −100.2, and −111.4 ppm. The intense peak at −91.6 ppm is assigned to Si(4Al) of SAPO-5, and the other peaks are due to Si(*n*Al, (4 − *n*)Si) environments. Thus, the peaks at −96, −100.2, and −111.4 ppm are assigned to Si(2Al, 2Si), Si(Al, 3Si), and Si(4Si), respectively.[37,38] These chemical shifts indicate that silicon atoms with different coordination environments are present in SAPO-5. The presence of these peaks also suggests that the silica-rich regions exist in the structure of SAPO-5. Especially, the intensity of the peak at −111.4 ppm is relatively high, which suggests that a relatively high content of Si(4Si) exist in the structure of SAPO-5. In the spectrum of VAPSO-5, except for the resonance peak of Si(4Al) at −91.6 ppm, the resonance peaks of Si(2Al, 2Si) and Si(4Si) at −96 and −110 ppm, respectively, are also observed, but the change in the intensity of each peak is different with the variation of vanadium content. Moreover, several shoulder peaks that are possibly due to amorphous SiO_2 are also observed in the region of ca. −80 to −90 ppm. These observations suggest that the introduction of vanadium into the molecular sieve can influence the relative content of differently coordinated silicon atoms in the framework. It also means that a competitive incorporation exists between vanadium and silicon with the addition of vanadium into the molecular sieves.

UV−Raman Spectra. UV−resonance Raman spectra of $AlPO_4$-5 and SAPO-5 are shown in Figure 6. In the spectrum of $AlPO_4$-5, Raman bands at 273, 407, 500, 643, 1060, and 1139 cm^{-1} are observed. The major vibrational region of interest lies in the 1500−100 cm^{-1} range. For aluminophosphate molecular sieves, this region can be divided into four primary parts: (1) the breathing modes of the opening channels that occur from 200−300 cm^{-1}; (2) the bending vibration region from 400−600 cm^{-1}; (3) the symmetric stretching modes of tetrahedral TO_4 from 600−900 cm^{-1}; and (4) the asymmetric stretching modes of tetrahedral PO_4 and AlO_4 units from 1000−1200 cm^{-1}. The Raman bands at 1139, 500, and 273 cm^{-1} in the spectra of $AlPO_4$-5 and SAPO-5 can be attributed to T−O stretching, T−O−T bending (T = Si, Al, or P), and ring-breathing vibrational modes, respectively.[39,40] They are the typical vibrations of aluminophosphate molecular sieves. Moreover, three other Raman bands at 600, 1077, and 1100 cm^{-1} are observed in the spectrum of SAPO-5 in comparison with the spectrum of $AlPO_4$-5. Similarly, the bands at 1077 and 1100 cm^{-1} are assigned to asymmetric stretching vibrations of the Si−O bond in Si−O−Al and Si−O−Si units, respectively. The band at 600 cm^{-1} can be assigned to the bending vibration of Si−O−Si units. These results suggest that several kinds of Si coordination environments exist in the framework of SAPO-5. Namely, the silicon atoms are coordinated not only in the Si(4Al) mode but also in the Si((4 − *n*)Al, *n*Si) (*n* = 1−4) mode in the framework of SAPO-5. This result is also confirmed by ^{29}Si MAS NMR spectra, in which the chemical shift of ∼110 ppm of Si(4Si) is evident.

UV−resonance Raman spectra of VAPO-5 and VAPSO-5 are shown in Figure 7. The UV−Raman spectra of $AlPO_4$-5 and VAPO-5 are significantly different. In the asymmetric stretching region, three new Raman bands at 930, 984, and 1038 cm^{-1} are observed. It is obviously that these bands are all associated with the vanadium species in the molecular sieves.[41] The Raman bands in the 900−1000 cm^{-1} region of supported vanadium oxides are usually attributed to hydrated polymerized vanadium oxides.[42] The terminal stretching mode found in alkali metavanadate that possesses polymeric chains of VO_4 units gives the Raman band at 960 cm^{-1}. Thus, the stronger bands at 930 and 984 cm^{-1} in the UV−Raman spectrum of VAPO-5 are

mainly due to polymerized vanadate oxide and can be assigned to the V═O stretching mode of polymerized vanadium oxides outside the framework and highly dispersed V_2O_5 particles, respectively. The weak shoulder at 1038 cm^{-1} in the spectrum of VAPO-5 is probably attributed to the V═O stretching mode of isolated vanadate. Because several types of polymerized vanadium oxides exist in the molecular sieves, the bands near 984 cm^{-1} are broad. Therefore, polymerized vanadium oxides, nanoparticle V_2O_5 crystallites, and vanadate species exist as the dominant vanadium species in VAPO-5, whereas the isolated framework vanadium species seem to be difficult to form in VAPO-5.

For the UV−Raman spectrum of VAPSO-5, it is worthwhile to note that three new Raman bands at 1028, 930, and 557 cm^{-1} appear when compared to the spectrum of SAPO-5 (Figure 6b). The band around 1040 cm^{-1} has been assigned to the V═O stretching vibration of monometric vanadyl species bound directly to the SiO_2 support.[13] The V═O stretching frequencies of VOF_3, $VOCl_3$, and $VOBr_3$ occur at 1053, 1035, and 1028 cm^{-1}, respectively.[43] The Raman band at 1035 cm^{-1} has also been assigned to the stretching frequency of a terminal V═O group bonded to the silicate MCM-41 host.[44] Very recently, the framework vanadium species in V-MCM-41 were also identified by UV−resonance Raman spectroscopy.[45] The characteristic Raman band at 1070 cm^{-1} due to a V═O vibration can be clearly detected on the basis of the UV−resonance Raman effect. Therefore, the band at 1028 cm^{-1} in the spectrum of VAPSO-5 is reasonably assigned to an isolated tetrahedral V═O group bonded to the silica host. The band at 557 cm^{-1} in the spectrum of VAPSO-5 corresponds to the bending vibration of a Si−O−V unit. This band indicates that the silicon atoms in the framework of SAPO-5 are connected to the isolated vanadium atoms. The band at 930 cm^{-1} is also observed, indicating that polymerized vanadium species coexist with isolated vanadium species in VAPSO-5.

Discussion

Since the first report in 1986,[5,6] the synthesis and characterization of VAPO and VAPSO molecular sieves have been studied extensively. There are differences among the results from these studies; therefore, different viewpoints were proposed on the basis of each set of results. Rigutto and van Beckkum[46] proposed that a monomeric vanadyl unit that occupies an Al site has either pyramidal or distorted octahedral coordination. Montes et al.[18] found that higher levels of substitution were possible in the $AlPO_4$-5 molecular sieve. They believed that V^{5+} was bonded to four Al sites through O atoms in oxidized VAPO-5. They also suggested that V^{4+} and V^{5+} would substitute for P^{5+} in the aluminophosphate framework. However, Lohse[47] pointed out that V is not capable of occupying tetrahedral sites as are Si and Co atoms in the $AlPO_4$ framework but that V could be fixed on the framework by condensation between VO^{2+} ions and hydroxyl groups. Chao et al.[44] also proposed that vanadyl ions in VAPO-5 are stabilized on the internal surface of the pores via condensation with the hydroxyl groups of Al−OH. Two questions that remain are whether the vanadium is incorporated into the framework and what kinds of coordination states of vanadium exist in the molecular sieve.[36]

From the TG and DTA profiles, it was found that the framework charge of VAPO-5 does not change greatly with the addition of vanadium atoms. This result seems to indicate that the vanadium atoms are not incorporated tetrahedrally into the framework. Otherwise, even if the vanadium replaces the Al or P atoms, the framework charge must be altered, thus leading to a different distribution of protonated amines and great changes in the TG and DTA profiles. However, the TG and DTA profiles of VAPSO-5 show that the amount of framework charge does increase with the addition of silicon and vanadium and that the more vanadium added, the higher the acidity. Only when vanadium and silicon are incorporated into the framework can the amount of framework charge be changed. Thus, this result tells us that vanadium is possibly incorporated into the framework of VAPSO-5 but is not incorporated into the framework of VAPO-5. This result also suggests that silicon has a great influence on the incorporation of vanadium.

This viewpoint can also be verified by the NMR results. Our ^{31}P NMR spectra suggest that only one kind of coordination mode of P, P(4Al) exists in the framework of VAPO-5 and VAPSO-5 (Figure 4). Thus, if the vanadium ions are connected to the framework, they are possibly not coordinated with P atoms. However, it is possible that vanadium ions are connected to Al via oxygen on the basis of the ^{27}Al NMR spectra. The appearance of the −12 ppm signal suggests that some aluminum atoms are in octahedral coordination that is formed by the framework tetrahedral aluminum that is coordinated to two other species. It is possible that the two other species are vanadium atoms or water molecules, so the vanadium ions in the VAPO-5 molecular sieve are connected to the framework by coordinating with the framework Al. This result is in agreement with the observation of Montes et al.[18]

The ^{29}Si NMR spectra of VAPSO-5 shows that the intensity of Si(4Al) in the framework decreases whereas the peaks in the silica-rich region change their intensities the content changes. It can be explained that the vanadium ions are mainly incorporated into the domain of SiO_2, and as a result, the number of Si−O−Al species decreases. DTA profiles of VAPSO-5 also suggest that the vanadium ions are incorporated into the silica domain. The incorporation of V(V) into silica will increase the amount of positive charge and decrease the amount of protonated triethylamine.

The method used to detect the vanadium species is Raman spectroscopy. A Raman spectrum can provide the vibrational modes of the zeolite framework, which was expected to give direct evidence of the vanadium ions incorporated into the framework. UV−Raman spectroscopy can not only avoid the interference of fluorescence but also improve the signal-to-noise ratio of Raman spectra.[20] Moreover, the resonance Raman effect can selectively enhance the intensity of the Raman signal by several orders of magnitude when the excitation laser is close to the electronic transition absorption of the sample.[21] Thus, the nature, location, and coordination state of vanadium species in VAPO-5 and VAPSO-5 could be observed clearly from UV−Raman spectra. In the UV−Raman spectrum of VAPO-5, Raman bands at 930, 984, and 1038 cm^{-1} are observed, indicating that polymerized vanadium oxides and nanoparticle V_2O_5 crystallites are mainly formed in VAPO-5. The polymerized vanadate, which is deduced by combining NMR results, is schematically shown in Figure 8a. This kind of vanadium species is formed by the condensation of vanadyl groups. The vanadyl ions in VAPO-5 are stabilized on the surface via condensation with the hydroxyl group of Al−OH, whereas upon calcination, two neighboring species will be linked by the hydroxyl condensation. Further condensation will form polymerized vanadium oxides and even bulk V_2O_5 crystallite.

In the UV−Raman spectrum of VAPSO-5, an intense Raman band at 1028 cm^{-1} is observed. It is obvious that the intensity of the band at 1028 cm^{-1} is much stronger than that of the other bands. The high intensity of this band owes to the resonance

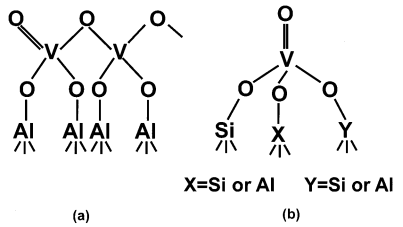

Figure 8. Coordination modes of (a) polymerized vanadate in VAPO-5 and (b) tetrahedrally coordinated framework vanadium species in VAPSO-5.

Raman enhancement. The excitation laser at 244 nm is close to the electronic absorption band of isolated vanadium species of VAPSO-5; therefore, the resonance Raman effect selectively enhances the Raman intensities of the vibrational modes related to the electronic transition. This is a piece of direct evidence for the incorporation of isolated mono-oxo vanadate species into the silica domain of the framework of VAPSO-5, which in turn provides convincing evidence for the isomorphous substitution of V into the lattice of the VAPSO-5 molecular sieve. In a word, the tetrahedral vanadium species are incorporated into the domain of silica in VAPSO-5 molecular sieves, which is depicted in Figure 8b.

Conclusions

Vanadium-containing aluminophosphate molecular sieves, VAPO-5 and VAPSO-5, were synthesized and characterized. VAPO-5 and VAPSO-5 can be synthesized with a relatively high concentration of vanadium in the synthesis gel. Calcination at high temperatures leads to the structural collapse of the molecular sieves with high vanadium content. The introduction of silicon increases the stability of the structure. The vanadium species formed in VAPO-5 and VAPSO-5 are found to be very different. The vanadium species in VAPO-5 are mainly the polymerized vanadium oxides together with small number of V_2O_5 particles. The vanadium species in VAPSO-5 are mainly in tetrahedral coordination and are incorporated into the framework of SAPO-5. The presence of silicon atoms in SAPO is beneficial to the formation of the isolated framework vanadium species in VAPSO-5.

Acknowledgment. This work was supported by the National Natural Science Foundation of China (grant no. 20073045) and the State Key Project for Basic Research from the Ministry of Science and Technology (grant no. 1999022407). We also thank Mr. Yue Yang and Mr. Xianchun Liu for XRD and NMR measurements.

References and Notes

(1) Haanepen, M. A.; Elemans-Mehring, M.; Van Hooff, J. H. C.; *Appl. Catal., A* **1997**, *152*, 203.
(2) Tuel, A.; Ben Taarit, Y. *J. Chem. Soc., Chem. Commun.* **1994**, 1667.
(3) Cambior, A. M.; Corma, A.; Perez-Pariente, *J. Chem. Soc., Chem. Commun.* **1993**, 557.
(4) Ulagappan, N.; Krishnasamy, V. *J. Chem. Soc., Chem. Commun.* **1995**, 373.
(5) Wilson, S. T.; Flanigen, E. M. U.S. Patent 4,567,029, 1986.
(6) Flanigen, E. M.; Lok, B. M.; Patton, R. L.; Wilson, S. T. *Pure Appl. Chem.* **1986**, *58*, 1351.
(7) Sheldon, R. A.; Dakka, J. *Catal. Today* **1994**, *19*, 215.
(8) Inui, T.; Phatanasri, S.; Matsuda, H. *J. Chem. Soc., Chem. Commun.* **1990**, 205.
(9) Wan, B.-Z.; Huang, K. *Appl. Catal.* **1991**, *73*, 113.
(10) Chen, J.; Thomas, J. M. *J. Chem. Soc., Chem. Commun.* **1994**, *603*, 475.
(11) Weckhuysen, B. M.; Rao, R. R.; Martens, J. A.; Schoonheydt, R. A. *Eur. J. Inorg. Chem.* **1999**, 565.
(12) Hartmann, M.; Kevan, L. *Chem. Rev.* **1999**, *99*, 635.
(13) Weckhuysen, B. M.; Vannijvel, I. P.; Schoonheydt, R. A. *Zeolites* **1995**, *15*, 482.
(14) Haanepen, M. J.; van Hooff, J. H. C. *Appl. Catal., A* **1997**, *152*, 183.
(15) Haanepen, M. J.; Elemans-Mehring, A. M.; van Hooff, J. H. C. *Appl. Catal., A* **1997**, *152*, 203.
(16) Blasco, T.; Concepción, P.; López Nieto, J. M.; Pérez-Pariente, J. *J. Catal.* **1995**, *152*, 1.
(17) Concepción, P.; López Nieto, J. M.; Mifsud, A.; Pérez-Pariente, J. *Appl. Catal., A* **1997**, *151*, 373.
(18) Montes, C.; Davis, M. E.; Murray, B.; Narayana, M. *J. Phys. Chem.* **1990**, *94*, 6431.
(19) Jhung, S. H.; Uh, Y.; Chon, H. *Appl. Catal.* **1990**, *62*, 61.
(20) Li, C.; Stair, P. C. *Stud. Catal. Surf. Sci.* **1996**, *36*, 119.
(21) Li, C.; Xiong, G.; Liu, J. K.; Ying, P. L.; Xin, Q.; Feng, Z. C. *J. Phys. Chem. B* **2001**, *105*, 2993.
(22) Li, C.; Xiong, G.; Xin, Q.; Liu, J. K.; Ying, P. L.; Feng, Z. C.; Li, J.; Yang, W. B.; Wang, Y. Z.; Wang, G. R.; Liu, X. R.; Lin, M.; Wang, X. Q.; Min, E. Z. *Angew. Chem., Int. Ed.* **1999**, *38*, 2220.
(23) Vassel, K. A.; Espenson, J. H. *Inorg. Chem.* **1994**, *33*, 5491.
(24) Singh, P. S.; Bandyopadhyah, R.; Rao, B. S. *J. Mol. Catal. A: Chem.* **1995**, *104*, 103.
(25) Franco, M. J.; Pariente; J. P.; Mifsud, A.; Blasco, T.; Sanz, J. *Zeolites* **1992**, *12*, 386.
(26) Blackwell, C. S.; Patton, R. L. *J. Phys. Chem.* **1988**, *92*, 3965.
(27) Franco, M. J.; Pérez-Pariente, J.; Blasco, T.; Sanz, J. *Zeolites* **1992**, *12*, 386.
(28) Zibrowius, B.; Lohse, U.; Richter-Mendau, J. *J. Chem. Soc., Faraday Trans.* **1991**, *87*, 1433.
(29) Blackwell, C. S.; Patton, R. L. *J. Phys. Chem.* **1988**, *92*, 3965.
(30) Blackwell, C. S.; Patton, R. L. *J. Phys. Chem.* **1984**, *88*, 6135.
(31) Meinhold, R. H.; Tapp, N. J. *Zeolites* **1991**, *11*, 401.
(32) Zubowa, H. L.; Alsdrof, E.; Fricke, R.; Neissendorfer, F.; Richeter-Mendau, J.; Schreier, D.; Zeigan, D.; Zibrowius, B. *J. Chem. Soc., Faraday Trans.* **1990**, *86*, 2307.
(33) Zibrowius, B.; Loffler, E.; Finger, F.; Sonntag, E.; Hunger, M.; Kornatowski, J. *Stud. Surf. Sci. Catal.* **1991**, *65*, 537.
(34) Zibrowius, B.; Lohse, U.; Richter-Mendau, J. *J. Chem. Soc., Faraday Trans.* **1991**, *87*, 1433.
(35) Parakash, A. M.; Unnikrishnan, S. *J. Chem. Soc., Faraday Trans.* **1994**, *90*, 2291.
(36) Frunza, L.; Pelgrims, J.; Leeman, H.; Van Der Voort, P.; Vansant, E. F.; Schoonheydt, R. A.; Weckhuysen, B. M. *J. Phys. Chem. B* **2001**, *105*, 2677−2686.
(37) Ashtekar, S.; Chilukuri, S. V. V.; Chakrabarty, D. K. *J. Phys. Chem.* **1994**, *98*, 4878.
(38) Deckman, H. W.; Creighton, J. A.; Buckley, R. G.; Newsam, J. M. *MRS Symp. Ser.* **1991**, *233*, 295.
(39) Holmes, A. J.; Kirkby, S. J.; Ozin, G. A.; Young, D. *J. Phys. Chem.* **1994**, *98*, 4677.
(40) Okuhara, T.; Inumaru, K.; Misono, M.; Matsubayashi, N. In *New Frontiers in Catalysis*, Proceeding of the 10th International Congress on Catalysis; Guczi, L., Solymosi, F., Tétényi, P., Eds.; Elsevier: New York, 1993; p 1767.
(41) Oyama, S. T.; Went, G. T.; Lewis, K. B.; Bell, A. T.; Somorjai, G. A. *J. Phys. Chem.* **1989**, *93*, 6786.
(42) Vuurman, M. A.; Wachs, I. E. *J. Phys. Chem.* **1992**, *96*, 5008.
(43) Selig, H.; Claassen, H. H. *J. Chem. Phys.* **1966**, *44*, 1404.
(44) Chao, K. J.; Wu, S. N.; Chang, H.; Lee, L. J.; Hu, S. F. *J. Phys. Chem. B* **1997**, *101*, 6341.
(45) Xiong, G.; Li, C.; Li, H. Y.; Xin, Q.; Feng, Z. C. *Chem. Commun.* **2000**, 677.
(46) Rigutto, M. S.; van Bekkum, H. *J. Mol. Catal.* **1993**, *81*, 1031.
(47) Lohse, U.; Brücker, A.; Kintscher, K.; Parlitz, B.; Schreier, E. *J. Chem. Soc., Faraday Trans.* **1995**, *91*, 1173.